P1.16

EFFECTS OF CONVECTIVELY GENERATED GRAVITY WAVE DRAG ON A NUMERICALLY PREDICTED HEAVY RAINFALL EVENT OCCURRED NEAR THE JIRI MOUNTAIN, KOREA

Hye-Yeong Chun* and Seung-Hee Sohn

Laboratory for Atmospheric Modeling Research/Department of Atmospheric Sciences
Yonsei University, Seoul, Korea

1. INTRODUCTION

Vertically propagating gravity waves can transport momentum to higher levels in the atmosphere, and they exert a significant amount of acceleration or deceleration on the mean flow at the level where wave breaking occurs. It is well known now that mountain-induced gravity wave drag is an important subgrid-scale dynamical process that should be included in general circulation models for the observed large-scale flows to be better simulated (Palmer et al, 1986). Recently, convectively generated gravity waves and their effects on large-scale flow have received a great attention in conjunction with a possible mechanism for quasi-biennial oscillation (QBO) (Alexander and Holton 1997). The association between gravity waves and convection has been known and exploited by glider pilots for many years. Observational evidence of convectively generated gravity waves have been reported by Hauf (1993) and Kuettner et al. (1987) above convective boundary layers in continental mid-latitudes and by Pfister et al. (1993) above deep convection in the tropics. Numerical simulations of convectively generated gravity waves and their characteristics have been investigated using two- or three-dimensional cloud-resolving models (e.g., Clark et al. 1986; Hauf and Clark 1989; Fovell et al. 1992; Piani et al. 2000).

There have been several attempts to parameterize gravity wave drag induced by convective cloud (GWDC) for use in large-scale models (e.g., Rind et al. 1988; Kershaw 1995; Chun and Baik 1998, CB98 hereafter). Recently, Chun et al. (2001) implemented GWDC parameterization scheme by CB98 in Yonsei University general circulation model and showed that the excessive westerly jet in Southern Hemisphere midlatitude of stratosphere can be alleviated significantly by GWDC process.

The numerical weather prediction (NWP) models are developing with higher horizontal and vertical resolutions by aid of improved computing ability and computational technology. However, operational NWP models with horizontal grid spacing of 10 x 10 km are still considered be fine scale. Because the smallest size of phenomena that can be resolved by a model is 4 δx , where δx is the horizontal grid spacing (Grasso 2000), individual cloud less than 40 km cannot be fully resolved in NWP models even with this fine resolution. Considering that gravity waves are mainly forced by individual convective cell, which has a horizontal scale on the order of 10 km, and dominant horizontal scale of convectively generated gravity waves is less than 40 km, GWDC process must be parameterized even in the find-scale NWP models. In this study, the GWD parameterization scheme proposed by CB98 is implemented into the operational version of Advanced Regional Prediction System (ARPS; Xue et al. 1995) in Korean Meteorological Administration (KMA), and effects of GWDC on mesoscale convective system are investigated. Numerical simulations are performed for a heavy rainfall event occurred near the Jiri mountain over the southwestern part of Korean Peninsular (KP) on 31 July, 1998.

*Corresponding author address: Prof. Hye-Yeong Chun, Department of Atmospheric Sciences, Yonsei University, Shinchon-dong, Seodaemun-ku, Seoul 120-749, Korea. Email : chy@atmos.yonsei.ac.kr

2. PARAMETERIZATION OF CONVECTIVELY INDUCED GRAVITY WAVE DRAG

The effects of subgrid-scale gravity wave drag can be included in the horizontal momentum equations by

$$\frac{\partial u}{\partial t} = -\frac{1}{\rho}\frac{\partial \tau_x}{\partial z} , \qquad (1)$$

$$\frac{\partial v}{\partial t} = -\frac{1}{\rho}\frac{\partial \tau_y}{\partial z} , \qquad (2)$$

where τ_x and τ_y are the zonal and meridional components of the wave stress and ρ is the air density. The parameterization of GWDC is essentially to find a vertical profile of τ_x and τ_y in each horizontal grid of the model. In CB98, vertical profile of wave stress was obtained from the cloud-top (reference level) to model top using linear saturation theory proposed by Lindzen (1981) based on Richardson number criterion. The cloud-top wave stress was calculated analytically from the analytically obtained thermally induced internal gravity wave solution. A procedure of CB98 shceme for calculating vertical profile of wave stress can be summarized as follows: 1) Calculate cloud-top wave stress vector based on the analytical formulation as

$$\vec{\tau}_{ct} = -\frac{\rho_{ct}\left|\vec{V}_{ct}\right|^2}{N\Delta x}\vec{V}_{ct} c_1 c_2{}^2 \mu_{ct}{}^2 , \qquad (3)$$

$$\mu_{ct} = \frac{g Q_0 a_1}{c_p N T \left|\vec{V}_{ct}\right|^2} , \qquad (4)$$

where Q_0 / c_p is the diabatic heating rate (Ks^{-1}) by subgrid-scale cumulus clouds, N the buoyancy frequency, T the temperature, $\vec{V}_{ct}$ the horizontal wind vector at cloud top, ρ the air density, Δx the horizontal grid size, g the gravitational acceleration, a_1 the approximate horizontal scale of effective cloud, and c_1 and c_2 are constants related to the horizontal and vertical structures of the diabatic forcing, respectively. 2) Calculate the minimum Richardson number including wave effect (Ri_{min}) at the level above cloud top. 3) Check whether wave breaking occurs based on the minimum Richardson number. That is, if $Ri_{min} \geq 1/4$ no wave breaking occurs, and τ at the level above cloud is set to the same value as on cloud top. If $Ri_{min} < 1/4$, wave breaking occurs, and calculate saturation wave stress which is paralle to the direction of cloud-top wave stress vector. 4) Repeat the previous steps 2) and 3) at the next higher level to the model top. 5) Determine the stress components in the x and y directions using the angle between x and y components of cloud-top wave stress vector. Detailed descript of CB98 GWDC parameterization scheme can be found in Chun et at. (2001).

3. NUMERICAL EXPERIMENTS

3.1 Model Configuration

The numerical model used in this study is the operational version of ARPS in KMA, which has one way nesting with horizontal resolution of 27 km for the coarse grid and 9 km for the fine grid. Figure 1 shows the terrain heights and configuration of model domain. The model contains 37 vertical levels utilizing a terrain following coordinate system. The first guess fields and boundary conditions for the 27 km run are provided by the Regional Data Analysis and Prediction System of the KMA. The model is initialized at 1200 UTC 31 July 1998 and all simulations are carried out for 12 hours. The initial data are obtained through ARPS Data Analysis System utilizing several data sets from different sources such as automatic weather stations, conventional surface and rawinsonde, and geostationary meteorological satellite.

3.2 Experimental Design

In order to investigate effects of GWDC on the numerically predicted mesoscale convective storms, two types of simulations are performed: control simulation without the GWDC parameterization and GWDC simulation with the GWDC parameterization. The observed data used for validation include rainfall data observed at synoptic stations and rain rate data observed by WSR-88D Doppler radar in Korea. The cumulus parameterization, most important part of GWDC parameterization, used in the present study is Kain-Fritsch (1993) scheme, and ice microphysics by Tao and Simpson (1993) and 1.5 TKE turbulent mixing scheme were consdered. All the physical processes considered in control and GWDC simulations are identical except for GWDC parameterization.

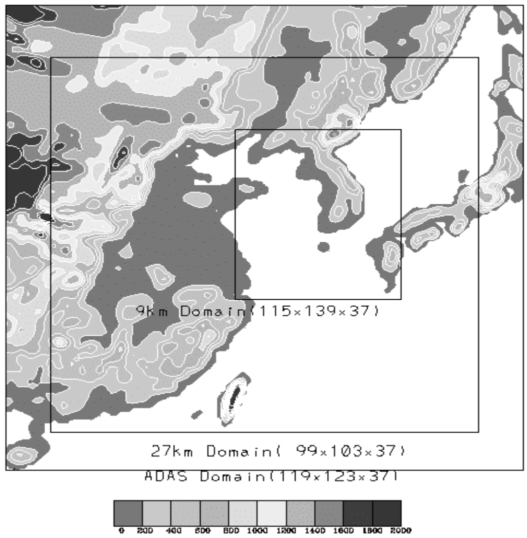

Fig.1. Terrain heights and configuration of the model domain.

4. RESULTS

4.1 Control Simulation

The model was able to reproduce most of the large-scale features related to monsoon fronts reasonably well under the given choice of parameterization schemes mentioned above, except that simulated results delayed about 1.5 hrs mainly due to the model spin-up process. The maximum values of 12-hr accumulated rainfall amount by course grid and fine grids are 108 mm and 148 mm, respectively. Figure 2 shows the simulated rain rate by the coarse and fine grid runs at 1800 UTC 31 July. Both results are reasonable compared with rain rate derived from radar observation (not shown) after considering 1.5 hr time lag. The fine-grid run with detailed terrain features could accurately simulate precipitation associated with Mt. Jiri located in the southwestern part of KP. The maximum value of 3-hr accumulated rainfall was matched very well to record-breaking observation value of 95 mm. It clearly shows that finer model resolution can significantly improve accurate prediction of precipitation over complex terrain in KP. However, problems of timing and locations of model precipitation still remain even in the fine-grid simulation.

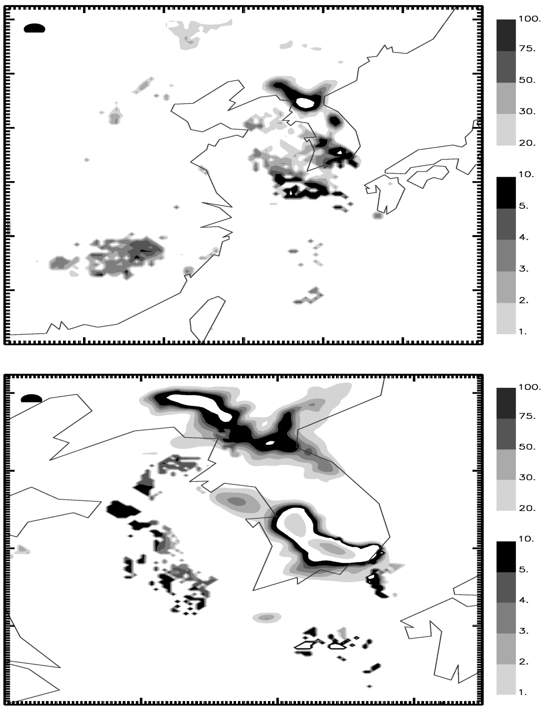

Fig. 2. Simulated rain rate for (a) 27 km and (b) 9 km grids at 1800 UTC 31 July 1998.

4.2 GWDC Simulation

The influence of GWDC on the large-scale wind can be estimated by magnitude of cloud-top wave stress because maximum change of the large-scale flow through the wave breaking directly depends on its magnitude. Figure 3 shows the cloud-top wave stress at 500 hPa and 200 hPa at 1400 UTC July 31. The maximum magnitude of gravity wave stress by midlevel clouds (cloud top at 500 hPa) is about 0.3 N m^{-2} in the Northern part of KP, while that by deep clouds (cloud top at 200 hPa) is about –4.5 N m^{-2} along the monsoon front located from the southeast of China to southwest coast of KP. The locations of middle and deep clouds are well matched in satellite observations. These values of maximum cloud-top wave stress are at least one order larger than those obtained in the general circulation model by Chun et al. (2001) mainly due to the larger value of diabatic heating rate (Q_0 / c_p) calculated in fine-resolution numerical model. Considering the large magnitude of wave stress, it can be expected that the GWDC process may have significant influence on mesoscale flow.

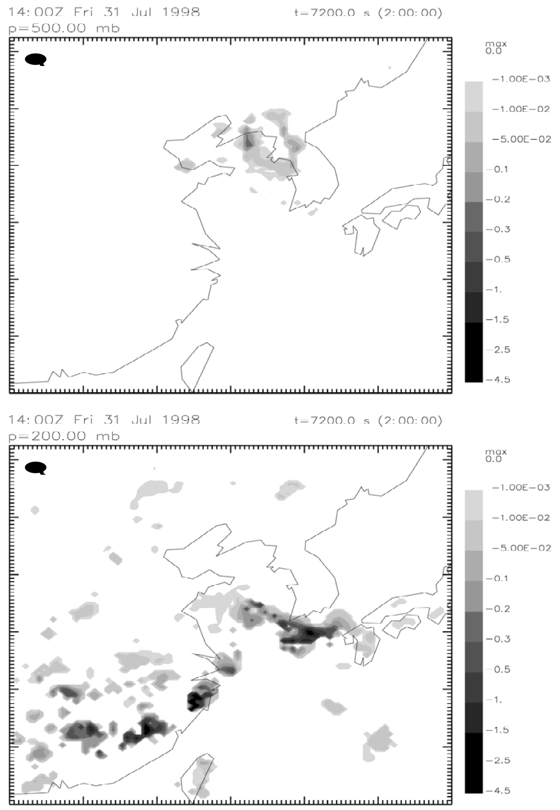

Fig. 3 Cloud-top wave stress at (a) 500 hPa and (b) 200 hPa.

Even though the magnitude of cloud-top wave stress by shallow clouds is relatively small compared with that by deep clouds, effect of GWDC parameterization is well presented in the low level wind field (not shown). The difference of 850 hPa wind vectors between the GWDC and control simulation indicates that horizontal wind are accelerated to northwest direction over most of model domain by GWDC parameterization. The maximum change of wind speed due to the GWDC parameterization at 850 hPa is about 10 m s^{-1}. Considering that mesoscale convective system around KP is developing and maintained by moisture supply from the southeast of China associated with monsoon circulation, enhanced low-level jet by GWDC process implies stronger and long-lasting convective system around KP. In addition, change of wind field in mid-troposphere provides different location of convective system. Considering that current NWP models have revealed some difficulties in predicting location of convective storms properly, including GWDC process may improve model performance through the accurate prediction of wind fields. This possibility is under investigation.

5 SUMMARY AND CONCLUSIONS

In this study, effects of GWDC parameterization on the numerically predicted mesoscale circulation were investigated by implementing the GWDC parameterization scheme proposed by CB98 into the operational version of ARPS in KMA. Numerical simulations were carried out for the heavy rainfall event occurred on July 31, 1998 near Mt. Jiri, located southwest coast of KP. Control simulation without GWDC parameterization could reproduce most of the large-scale features associated with monsoon circulation around KP reasonable well except that location and amount of heavy precipitation near Mt. Jiri were not properly predicted.

In GWDC simulation, cloud-top wave stress was distributed in the region of major convective clouds revealed in satellite observation. The magnitudes of maximum cloud-top wave stress were about 0.3 N m^{-2} by mid-level clouds (at 500 hPa) and 4.5 N m^{-2} by deep clouds (at 200 hPa). These values are at least one-order larger than those calculated from general circulation models mainly due to the larger value of diabatic heating rate obtained in high-resolution numerical model. The change of 850 hPa wind vector by GWDC process showed that southwesterly wind are accelerated by GWDC process in most of model domain. This implies that convective storms around KP developing along the monsoon front can be enhanced by stronger moisture supply from the southeast part of China under GWDC process. Detailed analysis of field difference between GWDC and control simulations is under investigation, and results will be presented in the conference.

Acknowledgments: This research was supported by the Korea Ministry of Science and Technology through National Research Laboratory Program and also by the Brain Korea 21 Program.

6. REFERENCES

Alexander, M. J., and J. R. Holton, 1997: A model study of zonal forcing in the equatorial stratosphere by convectively induced gravity waves. *J. Atmos. Sci.*, **54**, 408-419.

Chun, H.-Y., and J.-J. Baik, 1998: Momentum flux by thermally induced internal gravity waves and its approximation for large-scale models. *J. Atmos. Sci.*, **55**, 3299-3310.

_____, M.-D. Song, J.-W. Kim, and J.-J. Baik, 2001: Effects of gravity wave drag induced by cumulus convection on the atmospheric general circulation. *J. Atmos. Sci.*, **58**, 302-319.

Clark, T. L., Hauf, T. and Kuettner, J. P., 1986: Convectively forced internal gravity waves: Results from two-dimensional numerical experiments. *Quart. J. Roy. Meteor. Soc.*, **112**, 899-925.

Fovell, R., Durran, D. and Holton, J. R., 1992: Numerical simulations of convectively generated stratospheric gravity waves. *J. Atmos. Sci.*, **49**, 1427-1442.

Grasso, L. D., 2000: The differentitaion between grid spacing and resolution and their applications to numerical modeling. *Bull. Amer. Meteor. Soc.*, **81**, 579-580.

Hauf, T., 1993: Aircraft observation of convection waves - a case study. *Mon. Wea. Rev.*, **121**, 3282-3290.

Hauf , T. and Clark, T. L., 1989: Three- dimensional numerical experiments on convectively forced internal gravity waves. *Quart. J. Roy. Meteor. Soc.*, **115**, 309-333.

Kain, J. S. and J. M. Fritsch, 1993: Convective parameterization for mesoscale models: The Kain-Fritsch scheme. *The representation of Cumulus Convection in Numerical Models*, *Meteor. Monogr.,* No. 46, Amer. Meteor. Soc., 165-170.

Kershaw R., 1995: Parameterization of momentum transport by convectively generated gravity waves. *Quart. J. Roy. Meteor. Soc.*, **121**, 1023 -1040.

Kuettner , J. P., Hildebrand, P. A. and Clark, T. L., 1987: Convection waves : Observations of gravity wave systems over convectively active boundary layers. *Quart. J. Roy. Meteor. Soc.*, **113**, 445-467.

Lindzen, R. S., 1981: Turbulence and stress due to gravity wave and tidal breakdown. *J. Geophys. Res.*, **86**, 9707-9714.

Palmer, T. N., Shutts, G.J. and Swinbank, R., 1986: Alleviation of a systematic westerly bias in general circulation and numerical weather prediction models through an orographic gravity wave drag parameterization. *Quart. J. Roy. Meteor. Soc.*, **112**, 1001-1039.

Pfister, L., Scott, S. and Loewenstein, M., 1993: Mesoscale disturbances in the tropical stratosphere excited by convection: Observations and effects on the stratospheric momentum budget. *J. Atmos. Sci.*, **50**, 1058-1075

Piani, C., D. Durran, M. J. Alexander, and J. R. Holton, 2000: A numerical study of three-dimensional gravity waves triggered by deep tropical convection and their role in the dynamics of the QBO. *J. Atmos. Sci.*, **57**, 3689-3702.

Rind, D., R. Suozzo, N. K. Balachandran, A. Lacis, and G. Russel, 1988: The GISS global climate-middle atmosphere model. Part I: Model structure and climatology. *J. Atmos. Sci.*, **45**, 329-370.

Tao, W. K., and J. Simpson, 1993: Goddard cumulus ensemble model. Part 1: Model description. *Terr. Atmos. Ocea. Sci.,* 4, 35-72.

Xue, M., K. K. Droegemeier, V. Wong, A. Shapiro, and K. Brewster, 1995: *ARPS Version 4.0 Users' Guide*. Center for Analysis and Prediction of Storms, University of Oklahoma, 380 pp.